Cation−π Interactions: Structures and Energetics of Complexation of Na+ and K+ with the Aromatic Amino Acids, Phenylalanine, Tyrosine, and Tryptophan

Chunhai Ruan and M. T. Rodgers*

Contribution from the Department of Chemistry, Wayne State University, Detroit, Michigan 48202

Received March 24, 2004; E-mail: mrodgers@chem.wayne.edu

Abstract: Threshold collision-induced dissociation of M+(AAA) with Xe is studied using guided ion beam tandem mass spectrometry. M+ include the alkali metal ions Na+ and K+. The three aromatic amino acids are examined, AAA = phenylalanine, tyrosine, or tryptophan. In all cases, endothermic loss of the intact aromatic amino acid is the dominant reaction pathway. The threshold regions of the cross sections are interpreted to extract 0 and 298 K bond dissociation energies for the M+−AAA complexes after accounting for the effects of multiple ion−neutral collisions, internal energy of the reactant ions, and dissociation lifetimes. Density functional theory calculations at the B3LYP/6-31G* level of theory are used to determine the structures of the neutral aromatic amino acids and their complexes to Na+ and K+ and to provide molecular constants required for the thermochemical analysis of the experimental data. Theoretical bond dissociation energies are determined from single-point energy calculations at the B3LYP/6-311++G(3df,3pd) level using the B3LYP/6-31G* geometries. Good agreement between theory and experiment is found for all systems. The present results are compared to earlier studies of these systems performed via kinetic and equilibrium methods. The present results are also compared to the analogous Na+ and K+ complexes to glycine, benzene, phenol, and indole to elucidate the relative contributions that each of the functional components of these aromatic amino acids make to the overall binding in these complexes.

Introduction

The primary structure of peptides and proteins is determined by the covalent bonds that link amino acids together. The secondary, tertiary, and quaternary structures and the biochemical function of peptides and proteins are controlled by noncovalent interactions among the constituent amino acids, and with various metal or organic cations, substrates, and solvents. Because noncovalent interactions are generally much weaker than covalent bonds, they provide peptides and proteins with the flexibility to vary their structure and function with changes in the local environment. Despite the prominent roles that such noncovalent interactions play in the biochemistry of peptides and proteins, experimental determination of the strengths of such interactions is presently limited, primarily because of the numerous interactions involved in these systems. One means of addressing this lack of thermodynamic data is to quantitatively evaluate pairwise interactions between individual components of these systems, including more complex interactions that evolve in larger systems. These pairwise interactions can then be combined to provide accurate estimates for more complex systems.

Cation−π interactions are noncovalent binding forces that occur between cations and π systems. The cations involved in such interactions may include metal cations as well as complex organic cations, while the π system may vary between ethylene, the simplest π system, and complex single and multiple aromatic ring systems. The biological importance of such cation−π interactions has only recently been firmly established, and this

has aroused a great deal of interest in the study and characterization of these interactions in both model and real systems. Cation−π interactions are now recognized as playing equally important roles in the structure and function of peptides and proteins as other more conventional noncovalent forces, that is, hydrogen bonds, salt bridges, and hydrophobic forces. Reviews by Dougherty and co-workers provide detailed accounts of cation−π interactions, including both fundamental studies and their biological importance.[1,2]

Previous studies of cation−π interactions have established the importance of these forces in the stabilization of protein geometry.[1−8] The aromatic amino acids, phenylalanine (Phe), tyrosine (Tyr), and tryptophan (Trp), account for ~8.4% of all amino acids in proteins.[9] In an analysis of structures in the protein data bank, Gallivan and Dougherty found that one favorable cation−π interaction occurs for every 77 amino acid residues of protein length, and that 26% of all Trp residues are involved in energetically significant cation−π interactions.[10]

(1) Dougherty, D. A. *Science* **1996**, *271*, 163.
(2) Ma, J. C.; Dougherty, D. A. *Chem. Rev.* **1997**, *97*, 1303.
(3) DeVos, A. M.; Ultsch, M.; Kossiakoff, A. A. *Science* **1992**, *255*, 306.
(4) Karlin, A. *Curr. Opin. Neurobiol.* **1993**, *3*, 299.
(5) Stauffer, D. A.; Karlin, A. *Biochemistry* **1994**, *33*, 6840.
(6) Michell, J. B.; Nandi, C. L.; McDonald, I. K.; Thornton, J. M.; Price, S. L. *J. Mol. Biol.* **1994**, *239*, 315.
(7) Raves, M. L.; Harel, M.; Pang, Y. P.; Silman, I.; Kozikowski, A. P.; Sussman, J. L. *Nat. Struct. Biol.* **1997**, *4*, 57.
(8) Gokel, G. W.; DeWall, S. L.; Meadows, E. S. *Eur. J. Org. Chem.* **2000**, 2967.
(9) Meadows, E. S.; De Wall, S. L.; Barbour, L. J.; Gokel, G. W. *J. Am. Chem. Soc.* **2001**, *123*, 3092.

Cation−π interactions are also responsible for the functioning and selectivity in variable ion channels.[11−13] For example, the Shaker channel exhibits a selectivity for K+ over Na+ of 1000: 1.[14] Based on the sequences of a number of K+ channels, a highly conserved Gly−Tyr−Gly sequence (Tyr may be replaced by Phe in some cases) was found in the pore region of these K+ channels. Cation−π interaction between K+ and the aromatic side chain of Tyr was therefore proposed as being crucial for K+ selectivity.[15] This conclusion has now been confirmed by theoretical[16] and experimental results.[17] Previous studies have also established that cation−π interactions are important in biological recognition processes.[17,18]

As discussed above, one means of understanding and characterizing cation−π interactions operative in peptides and proteins is to quantitatively evaluate pairwise interactions between cations and the side chains of the aromatic amino acids as well as other functional groups present with which the cation might bind. These pairwise interactions can then be combined to provide an understanding of how such interactions evolve in peptides and proteins. Progress toward such an understanding of cation−π interactions in peptides and proteins has been achieved through studies of small model cation−π complexes. The great majority of these studies have involved the alkali metal cations, and in particular Na+ and K+, because these cations are very common in organisms and are the most biologically relevant metal cations.[2,8,19] The model π systems that have been experimentally investigated include: ethene,[20] benzene,[20−26] pyrrole,[27,28] toluene,[29] fluorobenzene,[30] aniline,[31] phenol,[32,33] anisole,[34] indole,[33,35] and naphthalene.[36] Model cation−π complexes have also been investigated via electronic structure theory.[2,20,25−40] These model studies have confirmed the elec-

trostatic nature of these interactions and have provided accurate bond dissociation energies (BDEs) for these systems. In addition, these studies have also revealed that cation−π interactions are dominated by the ion−quadrupole interaction which contributes ∼60−90% to the overall binding. Ion-induced dipole interactions have also been found to contribute to the binding, with greater contributions from these interactions for small cations.

To determine how simple cation−π interactions are influenced by the presence of other functional groups present in peptides and proteins, these model studies have been extended to the aromatic amino acids and small peptides. In a theoretical investigation of Phe, Tyr, and Trp and their interactions with Na+ and K+, Dunbar found several low-energy conformers of these species and characterized the binding energies of these complexes.[41] In a later study of the Na+(Phe) complex by Gapeev and Dunbar, a lower-energy conformation of Phe was found, suggesting that the binding in the Na+(Phe) and K+-(Phe) complexes is weaker than that reported in the earlier study.[42] Siu and co-workers compared the relative stability of charge solvated (CS) and zwitterionic forms of Na+(Phe) and confirmed the most stable conformer of Na+(Phe) found by Gapeev and Dunbar.[43] They also found that the aromatic side chain is important for stabilizing the CS form of Na+(Phe). There have also been a few experimental investigations of the binding of Na+ and K+ to the aromatic amino acids. Wesdemiotis and co-workers used the kinetic method to determine the binding energies of Na+ and K+ to Phe, Tyr, and Trp.[44] However, the binding energies determined in this work showed very poor agreement with the theoretical values found by Dunbar. In the study by Gapeev and Dunbar, they used ligand exchange equilibria to determine the binding energy of Na+-(Phe).[42] The binding energy measured for the Na+(Phe) complex showed much better agreement with the new theoretical value based upon the more stable conformation found for Phe. The complexes of Na+ with Phe, Tyr, and Trp were later re-examined using the kinetic method by Kish et al. and were found to be in much better agreement with the theoretical values found by Dunbar.[45] In a more recent ligand exchange equilibria study, Gapeev and Dunbar measured the Na+(Trp) binding affinity and remeasured the Na+(Phe) binding affinity. The remeasured value for Na+(Phe) was 8 kJ/mol larger than that found in their previous study and therefore in even better agreement with theory than their previous determination. The value determined for Na+(Trp) was somewhat lower than the theoretical values.[46]

Interactions of Phe, Tyr, and Trp with other metal cations have also been investigated. Binding energies of Ag+ and Cu+ to Phe, Tyr and Trp have been determined using the kinetic method.[47,48] However, these transition metal−π interactions are usually not categorized as cation−π interactions as a result of the significant d orbital participation in the binding.[2] In a study of the CID behavior of alkaline earth metal cations (Ca2+, Sr2+, and Ba2+) bound to peptides, Hu and Sorensen concluded that

(10) Gallivan, J. P.; Dougherty, D. A. *Proc. Natl. Acad. Sci. U.S.A.* **1999**, *96*, 9459.
(11) Kumpf, R. A.; Dougherty, D. A. *Science* **1993**, *261*, 5129.
(12) Zhong, W.; Gallivan, J. P.; Zhang, Y.; Li, L.; Sester, H. A.; Dougherty, D. A. *Proc. Natl. Acad. Sci. U.S.A.* **1998**, *95*, 12088.
(13) Donini, O.; Weaver, D. F. *J. Comput. Chem.* **1998**, *19*, 1515.
(14) Miller, C. *Science* **1991**, *252*, 1092.
(15) Heginbotham, L.; Mackinnon, R. *Neuron* **1992**, *8*, 483.
(16) Kumpf, R. A.; Dougherty, D. A. *Science* **1993**, *261*, 1708.
(17) Cabarcos, O. M.; Weinheimer, C. J.; Lisy, J. M. *J. Chem. Phys.* **1999**, *110*, 8429.
(18) Bond, A. H.; Dietz, M. L.; Rogers, R. D.; Eds. *Metal-Ion Separation and Preconcentration*; ACS Symposium Series 716; American Chemical Society: Washington, DC, 1999.
(19) Lippard, S. J.; Berg, J. M.; Eds. *Principles of Bioinorganic Chemistry*; University Science Books: Mill Valley, CA, 1994.
(20) Armentrout, P. B.; Rodgers, M. T. *J. Phys. Chem. A* **2000**, *104*, 2238.
(21) Sunner, J.; Nishizawa, K.; Kebarle, P. *J. Phys. Chem.* **1981**, *85*, 1814.
(22) Guo, B. C.; Purnell, J. W.; Castleman, A. W. *Chem. Phys. Lett.* **1990**, *168*, 155.
(23) Woodin, R. L.; Beauchamp, J. L. *J. Am. Chem. Soc.* **1978**, *100*, 501.
(24) Taft, R. W.; Anvia, F.; Gal, J.-F.; Walsh, S.; Capon, M.; Holmes, M. C.; Hosn, K.; Oloumi, G.; Vasanwala, R.; Yazdani, S. *Pure Appl. Chem.* **1990**, *62*, 17.
(25) Amicangelo, J. C.; Armentrout, P. B. *J. Phys. Chem. A* **2000**, *104*, 11420.
(26) Amincangelo, J. C.; Armentrout, P. B. *Int. J. Mass Spectrom.* **2001**, *212*, 301.
(27) Gapeev, A.; Yang, C.-Y.; Klippenstein, S. J.; Dunbar, R. C. *J. Phys. Chem. A* **2000**, *104*, 3246.
(28) Huang, H.; Rodgers, M. T. *J. Phys. Chem. A* **2002**, *106*, 4277.
(29) Amunugama, R.; Rodgers, M. T. *J. Phys. Chem. A* **2002**, *106*, 5529.
(30) Amunugama, R.; Rodgers, M. T. *J. Phys. Chem. A* **2002**, *106*, 9092.
(31) Amunugama, R.; Rodgers, M. T. *Int. J. Mass Spectrom.* **2003**, *227*, 339.
(32) Amunugama, R.; Rodgers, M. T. *J. Phys. Chem. A* **2002**, *106*, 9718.
(33) Ryzhov, V.; Dunbar, R. C. *J. Am. Chem. Soc.* **1999**, *121*, 2259.
(34) Amunugama, R.; Rodgers, M. T. *Int. J. Mass Spectrom.* **2003**, *222*, 431.
(35) Ruan, C.; Rodgers, M. T. *J. Phys. Chem. A*, in preparation.
(36) Amunugama, R.; Rodgers, M. T. *Int. J. Mass Spectrom.* **2003**, *227*, 1.
(37) Feller, D.; Dixon, D. A.; Nicholas, J. B. *J. Phys. Chem. A* **2000**, *104*, 11414.
(38) Tsuzuki, S.; Yoshida, M.; Uchimaru, T.; Mikami, M. *J. Phys. Chem. A* **2001**, *105*, 769.
(39) Mecozzi, S.; West, R. C., Jr.; Dougherty, D. A. *J. Am. Chem. Soc.* **1996**, *118*, 2307.
(40) Dunbar, R. C. *J. Phys. Chem. A* **1998**, *102*, 8946.

(41) Dunbar, R. C. *J. Phys. Chem. A* **2000**, *104*, 8067.
(42) Gapeev, A.; Dunbar, R. C. *J. Am. Chem. Soc.* **2001**, *123*, 8360.
(43) Siu, F. M.; Ma, N. L.; Tsang, C. W. *J. Am. Chem. Soc.* **2001**, *123*, 3397.
(44) Ryzhov, V.; Dunbar, R. C.; Cerda, B.; Wesdemiotis, C. *J. Am. Soc. Mass Spectrom.* **2000**, *11*, 1037.
(45) Kish, M. M.; Ohanessian, G.; Wesdemiotis, C. *Int. J. Mass Spectrom.* **2003**, *227*, 509.
(46) Gapeev, A.; Dunbar, R. C. *Int. J. Mass Spectrom.* **2003**, *228*, 825.
(47) Lee, V. W.-M.; Li, H.; Lau, T.-C.; Guevremont, R.; Siu, k. W. M. *J. Am. Soc. Mass Spectrom.* **1998**, *9*, 760.
(48) Cerda, B. A.; Wesdemiotis, C. *J. Am. Chem. Soc.* **1995**, *117*, 9734.

these cations interact with the aromatic amino acids more strongly than to other amino acids. This conclusion was supported by the observation of abundant metal-containing a_n fragments arising from cleavages adjacent to aromatic amino acid residues in the CID mass spectra of the alkaline earth metal cation bound peptides.[49]

In the present paper, we examine the interactions between Na^+ and K^+ and the aromatic amino acids, Phe, Tyr, and Trp, using threshold collision-induced dissociation (TCID) techniques in a guided ion beam tandem mass spectrometer and quantum-chemical calculations. The driving force behind our re-examination of these systems is to clarify the nature and trends of these cation–π interactions and provide accurate thermochemical measurements that provide absolute anchors for the alkali metal cation affinity scales.

Experimental Section

General Procedures. Cross sections for collision-induced dissociation of $M^+(AAA)$, where $M^+ = Na^+$ and K^+ and AAA = Phe, Tyr, or Trp, are measured using a guided ion beam tandem mass spectrometer that has been described in detail previously.[50] The $M^+(AAA)$ complexes are generated in a flow tube ion source by condensation of the alkali metal cation and neutral aromatic amino acid. These complexes are collisionally stabilized and thermalized by in excess of 10^5 collisions with the He and Ar bath gases such that the internal energies of the ions emanating from the source region are well described by a Maxwell–Boltzmann distribution at room temperature. The ions are extracted from the source, accelerated, and focused into a magnetic sector momentum analyzer for mass analysis. Mass-selected ions are decelerated to a desired kinetic energy and focused into an octopole ion guide. The octopole passes through a static gas cell containing Xe at low pressures (0.05–0.20 mTorr), to ensure that multiple ion–neutral collisions are improbable. The octopole ion guide acts as an efficient trap for ions in the radial direction. Therefore, loss of scattered reactant and product ions in the octopole region is almost entirely eliminated.[51] Xe is used here, and in general for all of our CID measurements, because it is heavy and polarizable and therefore leads to more efficient kinetic to internal energy transfer in the CID process.[52–54] Product and unreacted reactant ions drift to the end of the octopole where they are focused into a quadrupole mass filter for mass analysis and subsequently detected with a secondary electron scintillation detector and standard pulse counting techniques.

Data Handling. Measured ion intensities are converted to absolute cross sections using a Beers' law analysis as described previously.[55] Absolute uncertainties in cross-section magnitudes are estimated to be ±20%, which are largely the result of errors in the pressure measurement and the length of the interaction region. Relative uncertainties are approximately ±5%.

Ion kinetic energies in the laboratory frame, E_{lab}, are converted to energies in the center of mass frame, E_{CM}, using the formula $E_{CM} = E_{lab}m/(m + M)$, where M and m are the masses of the ionic and neutral reactants, respectively. All energies reported below are in the CM frame unless otherwise noted. The absolute zero and distribution of the ion kinetic energies are determined using the octopole ion guide as a retarding potential analyzer as previously described.[55] The distribution of ion kinetic energies is nearly Gaussian with a fwhm between 0.2 and 0.4 eV (lab) for these experiments. The uncertainty in the absolute energy scale is ±0.05 eV (lab).

Pressure-dependent studies of all CID cross sections examined here were performed because multiple collisions can influence the shape of CID cross sections and the threshold regions are most sensitive to these effects. Data free from pressure effects are obtained by extrapolating to zero reactant pressure, as described previously.[56] Thus, cross sections subjected to analysis are the result of single bimolecular encounters.

Quantum-Chemical Calculations. To obtain model structures, vibrational frequencies, and energetics for Phe, Tyr, and Trp and their complexes to Na^+ and K^+, density functional theory (DFT) calculations were performed using the Gaussian 98 suite of programs.[57] Geometry optimizations were performed at the B3LYP/6-31G* level.[58,59] Vibrational analyses of the geometry-optimized structures were performed to determine the vibrational frequencies and rotational constants of the optimized species for use in modeling the CID data. DFT theory, and in particular the B3LYP and B3P86 functionals, has proven very reliable for the determination of vibrational frequencies. The frequencies thus calculated were scaled by a factor of 0.9804.[60] The scaled vibrational frequencies are available as Supporting Information and are listed in Table 1S. Table 2S lists the rotational constants. Single-point energy calculations with an extended basis set, B3LYP/6-311++G(3df,3pd), were performed using the B3LYP/6-31G* optimized geometries. To obtain more accurate energetics, zero-point energy (ZPE) corrections were applied and basis set superposition errors (BSSE) were subtracted from the computed BDEs using the counterpoise approach.[61,62]

As a result of the flexibility of the AAAs and the multiple favorable metal ion binding sites, several low-energy conformations of these species are possible. Therefore, we carefully consider various possible conformations of the neutral AAAs and the $M^+(AAA)$ complexes to determine the ground-state conformations of these species. Because these species have also been examined in several previous theoretical studies,[41–43] we limit our discussion to the lowest-energy conformations found in our work.

To assess the dependence of our theoretical results on the level of theory employed for geometry optimization, we also performed geometry optimizations of the $Na^+(Phe)$ complex at the B3LYP/6-31G, B3LYP/6-31+G, and B3LYP/6-31+G* levels of theory. Single-point energy calculations with the extended basis set, B3LYP/6-311++G-(3df,3pd), were performed using these optimized structures to determine the influence of the optimized structure on the stability of the complex.

Thermochemical Analysis. The threshold regions of the CID cross sections are modeled using eq 1,

$$\sigma(E) = \sigma_0 \sum g_i(E + E_i - E_0)^n/E \qquad (1)$$

where σ_0 is an energy independent scaling factor, E is the relative

(49) Hu, P.; Sorensen, C.; Gross, M. L. *J. Am. Soc. Mass Spectrom.* **1995**, *6*, 1079.
(50) Rodgers, M. T. *J. Phys. Chem. A* **2001**, *105*, 2374.
(51) Teloy, E.; Gerlich, D. *Chem. Phys.* **1974**, *4*, 417. Gerlich, D. Diplomarbeit, University of Freiburg, Federal Republic of Germany, 1971. Gerlich, D. In *State-Selected and State-to-State Ion–Molecule Reaction Dynamics, Part I, Experiment*; Ng, C.-Y., Baer, M., Eds.; Advances in Chemical Physics Series; Wiley: New York, 1992; Vol. 82, p 1.
(52) Dalleska, N. F.; Honma, K.; Armentrout, P. B. *J. Am. Chem. Soc.* **1993**, *115*, 12125.
(53) Aristov, N.; Armentrout, P. B. *J. Phys. Chem.* **1986**, *90*, 5135.
(54) Hales, D. A.; Armentrout, P. B. *J. Cluster Sci.* **1990**, *1*, 127.
(55) Ervin, K. M.; Armentrout, P. B. *J. Chem. Phys.* **1985**, *83*, 166.

(56) Dalleska, N. F.; Honma, K.; Sunderlin, L. S.; Armentrout, P. B. *J. Am. Chem. Soc.* **1994**, *116*, 3519.
(57) Frisch, M. J.; Trucks, G. W.; Schlegel, H. B.; Scuseria, G. E.; Robb, M. A.; Cheeseman, J. R.; Zakrzewski, V. G.; Montgomery, J. A., Jr.; Stratmann, R. E.; Burant, J. C.; Dapprich, S.; Millam, J. M.; Daniels, A. D.; Kudin, K. N.; Strain, M. C.; Farkas, O.; Tomasi, J.; Barone, V.; Cossi, M.; Cammi, R.; Mennucci, B.; Pomelli, C.; Adamo, C.; Clifford, S.; Ochterski, J.; Petersson, G. A.; Ayala, P. Y.; Cui, Q.; Morokuma, K.; Malick, D. K.; Rabuck, A. D.; Raghavachari, K.; Foresman, J. B.; Cioslowski, J.; Ortiz, J. V.; Stefanov, B. B.; Liu, G.; Liashenko, A.; Piskorz, P.; Komaromi, I.; Gomperts, R.; Martin, R. L.; Fox, D. J.; Keith, T.; Al-Laham, M. A.; Peng, C. Y.; Nanayakkara, A.; Gonzalez, C.; Challacombe, M.; Gill, P. M. W.; Johnson, B.; Chen, W.; Wong, M. W.; Andres, J. L.; Gonzales, C.; Head-Gordon, M.; Replogle, E. S.; Pople, J. A. *Gaussian 98*, revision A.11; Gaussian, Inc.: Pittsburgh, PA, 1998.
(58) Becke, A. D. *J. Chem. Phys.* **1993**, *98*, 5648.
(59) Lee, C.; Yang, W.; Parr, R. G. *Phys. Rev. B* **1988**, *37*, 785.
(60) Foresman, J. B.; Frisch, M. J. *Exploring Chemistry with Electronic Structure Methods*, 2nd ed.; Gaussian: Pittsburgh, PA, 1996.
(61) Boys, S. F.; Bernardi, R. *Mol. Phys.* **1979**, *19*, 553.
(62) van Duijneveldt, F. B.; van Duijneveldt-van de Rijdt, J. G. C. M.; van Lenthe, J. H. *Chem. Rev.* **1994**, *94*, 1873.

translational energy of the reactants, E_0 is the threshold for reaction of the ground electronic and ro-vibrational state, and n is an adjustable parameter that describes the efficiency of kinetic to internal energy transfer.[63] The summation is over the ro-vibrational states of the reactant ions, i, where E_i is the excitation energy of each state and g_i is the population of those states ($\sum g_i = 1$). The populations of excited ro-vibrational levels are not negligible even at 298 K as a result of the many low-frequency modes present in these ions. The relative reactivity of all ro-vibrational states, as reflected by σ_0 and n, is assumed to be equivalent.

The Beyer–Swinehart algorithm is used to evaluate the density of the ro-vibrational states,[64] and the relative populations, g_i, are calculated for a Maxwell–Boltzmann distribution at 298 K, the temperature appropriate for the reactants. The vibrational frequencies of the reactant complexes are determined from DFT calculations as discussed in the Quantum-Chemical Calculations section. The average internal energies at 298 K of the neutral AAAs and $M^+(AAA)$ complexes are also given in Table 1S. We have estimated the sensitivity of our analysis to the deviations from the true frequencies by scaling the calculated frequencies to encompass the range of average scaling factors needed to bring calculated frequencies into agreement with experimentally determined frequencies found by Pople et al.[65] Thus, the originally calculated and appropriately scaled vibrational frequencies were increased and decreased by 10%. The corresponding change in the average vibrational energy is taken to be an estimate of one standard deviation of the uncertainty in vibrational energy (Table 1S) and is included in the uncertainties listed with the E_0 values.

As the complexity of the reactant ions increases, there is an increased probability that the CID reaction does not occur on the experimental time scale, ~10^{-4} s in our apparatus. All CID processes occurring faster than this are observed. However, as the lifetime of the energized molecule (EM) approaches this limit, the apparent CID threshold will shift to higher energies, a so-called kinetic shift. The extent of the kinetic shift ultimately depends on the sensitivity of the apparatus as well as on the experimental time scale available. This kinetic shift is quantified and corrected for in our analysis by including statistical theories for unimolecular dissociation, specifically Rice–Ramsperger–Kassel–Marcus (RRKM) theory, into eq 1 as described in detail elsewhere.[66,67] This requires sets of ro-vibrational frequencies appropriate for the EM and the transition states (TSs) leading to dissociation. The most appropriate TS for CID of noncovalently bound complexes, such as those examined here, is a loose phase space limit (PSL) in which the TS occurs at the centrifugal barrier for dissociation. Therefore, the TS is product-like and modeled using the ro-vibrational frequencies of the products.[66] The ro-vibrational frequencies of the EMs and TSs of the $M^+(AAA)$ complexes are given in Tables 1S and 2S. The necessity of including corrections for kinetic shifts has been firmly established in previous studies, where kinetic shifts have been observed when the total number of heavy atoms in the complex exceeds five and when the bond being broken is stronger than ~100 kJ/mol. Kinetic shifts increase in magnitude with the size and complexity of the reactant ions and the strength of the bond cleaved. As an extreme case, a kinetic shift of 4.30 eV was determined for the $Na^+(18$-crown-$6)$ system where the accuracy of the measured BDE was verified by comparison with high level ab initio calculations.[68] The $M^+(AAA)$ complexes examined
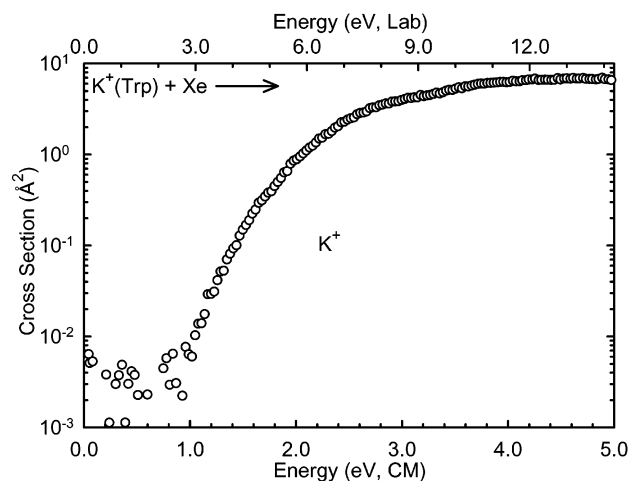

Figure 1. Cross section for the collision-induced dissociation of the K^+-(Trp) complex with Xe as a function of collision energy in the center-of-mass frame (lower *x*-axis) and laboratory frame (upper *x*-axis). Data for the M^+ product are shown for a Xe pressure of 0.2 mTorr.

here possess fewer heavy atoms (13 to 16 vs 19) and involve less chelation interactions (2 to 3 vs 6) and are therefore expected to exhibit significantly smaller kinetic shifts. At present, it is unclear how complex the system can become before the accuracy of our lifetime analysis will be compromised, but it seems clear that this limit is not approached in the present work.

The model represented by eq 1 is expected to be appropriate for translationally driven reactions[69] and has been found to reproduce reaction cross sections well in a number of previous studies of CID processes. The model of eq 1 is convoluted with the kinetic energy distributions of both reactants, and a nonlinear least-squares analysis of the data is performed to give optimized values for the parameters σ_0, E_0, and n. The error associated with the measurement of E_0 is estimated from the range of threshold values determined for the eight zero-pressure extrapolated data sets, variations associated with uncertainties in the vibrational frequencies, and the error in the absolute energy scale, 0.05 eV (lab). For analyses that include the RRKM lifetime analysis, the uncertainties in the reported $E_0(PSL)$ values also include the effects of increasing and decreasing the time assumed available for dissociation (~10^{-4} s) by a factor of 2.

Equation 1 explicitly includes the internal energy of the ion, E_i. All energy available is treated statistically because the ro-vibrational energy of the reactants is redistributed throughout the ion upon impact with Xe. Because the CID processes examined here are simple noncovalent bond cleavage reactions, the $E_0(PSL)$ values determined from analysis with eq 1 can be equated to 0 K BDEs.[70,71] The accuracy of the thermochemistry obtained by this modeling procedure has been verified for many systems by comparing when possible to values derived by other experimental techniques and to ab initio calculations. Absolute BDEs in the range from ~10 to ~400 kJ/mol can be determined accurately using TCID techniques.[72]

Results

Cross Sections for Collision-Induced Dissociation. Experimental cross sections were obtained for the interaction of Xe with six $M^+(AAA)$ complexes, where $M^+ = Na^+$ and K^+ and AAA = Phe, Tyr, and Trp. Figure 1 shows representative data for the K^+(Trp) complex. The other five $M^+(AAA)$ complexes exhibit similar behavior and are shown in Figure 1S in the

(63) Muntean, F.; Armentrout, P. B. *J. Chem. Phys.* **2001**, *115*, 1213.
(64) Beyer, T. S.; Swinehart, D. F. *Commun. ACM* **1973**, *16*, 379. Stein, S. E.; Rabinovitch, B. S. *J. Chem. Phys.* **1973**, *58*, 2438–2445; *Chem. Phys. Lett.* **1977**, *49*, 183.
(65) Pople, J. A.; Schlegel, H. B.; Raghavachari, K.; DeFrees, D. J.; Binkley, J. F.; Frisch, M. J.; Whitesides, R. F.; Hout, R. F.; Hehre, W. J. *Int. J. Quantum Chem. Symp.* **1981**, *15*, 269. DeFrees, D. J.; McLean, A. D. *J. Chem. Phys.* **1985**, *82*, 333.
(66) Rodgers, M. T.; Ervin, K. M.; Armentrout, P. B. *J. Chem. Phys.* **1997**, *106*, 4499.
(67) Khan, F. A.; Clemmer, D. E.; Schultz, R. H.; Armentrout, P. B. *J. Phys. Chem.* **1993**, *97*, 7978.
(68) More, M. B.; Ray, D.; Armentrout, P. B. *J. Am. Chem. Soc.* **1999**, *121*, 417.

(69) Chesnavich, W. J.; Bowers, M. T. *J. Phys. Chem.* **1979**, *83*, 900.
(70) See, for example, Figure 1 in: Dalleska, N. F.; Honma, K.; Armentrout, P. B. *J. Am. Chem. Soc.* **1993**, *115*, 12125.
(71) Armentrout, P. B.; Simons, J. *J. Am. Chem. Soc.* **1992**, *114*, 8627.
(72) Rodgers, M. T.; Armentrout, P. B. *Mass Spectrom. Rev.* **2000**, *19*, 215.

Table 1. Fitting Parameters, Threshold Dissociation Energies at 0 K, and Entropies of Activation at 1000 K of $M^+(AAA)^a$

reactant ion	$\sigma_0{}^b$	n^b	$E_0{}^c$ (eV)	E_0(PSL) (eV)	kinetic shift (eV)	$\Delta S^\ddagger$ (PSL) $(J\ mol^{-1}\ K^{-1})$
Na^+(Phe)	3.8 (0.4)	0.98 (0.05)	3.02 (0.07)	2.13 (0.07)	0.89	61 (2)
Na^+(Tyr)	2.3 (0.5)	1.17 (0.25)	3.19 (0.18)	2.17 (0.10)	1.02	61 (2)
Na^+(Trp)	2.6 (0.1)	0.97 (0.01)	3.62 (0.05)	2.25 (0.08)	1.37	56 (3)
K^+(Phe)	5.7 (0.4)	1.44 (0.06)	1.95 (0.06)	1.56 (0.06)	0.39	57 (2)
K^+(Tyr)	3.7 (1.0)	1.75 (0.22)	2.14 (0.15)	1.61 (0.09)	0.53	56 (3)
K^+(Trp)	9.9 (0.5)	0.82 (0.08)	2.52 (0.06)	1.71 (0.06)	0.81	48 (3)

^{a} Uncertainties are listed in parentheses. ^{b} Average values for the loose PSL transition state. ^{c} No RRKM analysis.

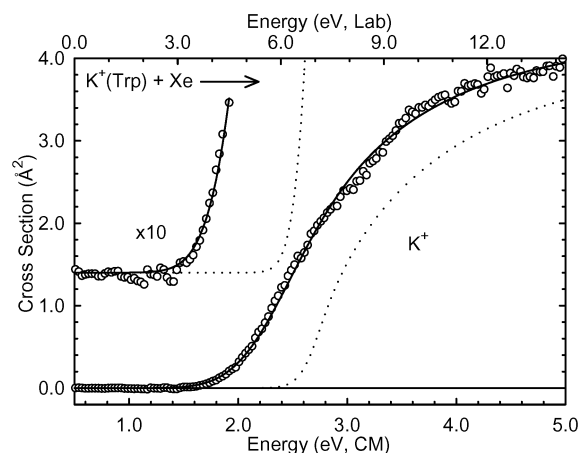**Figure 2.** Zero pressure extrapolated cross section for the collision-induced dissociation of the K^+(Trp) complex with Xe in the threshold region as a function of kinetic energy in the center-of-mass frame (lower *x*-axis) and laboratory frame (upper *x*-axis). The solid line shows the best fit to the data using eq 1 convoluted over the neutral and ion kinetic and internal energy distributions. The dotted line shows the model cross sections in the absence of experimental kinetic energy broadening for reactants with an internal energy corresponding to 0 K.

Supporting Information. The most favorable process for all complexes is the loss of the intact aromatic amino acid in the CID reactions 2.

$$M^+(AAA) + Xe \rightarrow M^+ + AAA + Xe \qquad (2)$$
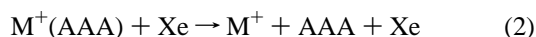
The magnitudes of the cross sections increase in size from Na^+ to K^+. This is largely because the thresholds decrease in this same order. No other products were observed in any of these systems except for the K^+(Phe) complex, where ligand exchange was observed to form KXe^+. However, the cross section for this product is more than 2 orders of magnitude smaller than that of the primary K^+ product. It is likely that this process occurs for all complexes, but that the signal-to-noise in the other experiments was not sufficient to differentiate the M^+Xe product from background noise.

Threshold Analysis. The model of eq 1 was used to analyze the thresholds for reactions 2 in six $M^+(AAA)$ systems. The results of these analyses are provided in Table 1, and representative results are shown in Figure 2 for the K^+(Trp) complex. The analyses for the other five $M^+(AAA)$ complexes are shown in Figure 2S in the Supporting Information. In all cases, the experimental cross sections for CID reactions 2 are accurately reproduced using a loose PSL TS model.[66] Previous work has shown that this model provides the most accurate assessment of the kinetic shifts for CID processes of electrostatically bound

Table 2. Enthalpies of Metal Ion Binding to Phe, Tyr, and Trp at 0 K in kJ/mol

reactant ion	experimental results		theoretical results	
	$TCID^a$	literature	$B3LYP^b$	literature
Na^+(Phe)	205.5 (6.8)	187 (8)^c	196.0	201^e
		195 (8)^d		188^d
				190^f
Na^+(Tyr)	209.4 (9.6)		198.2	202^e
Na^+(Trp)	217.1 (7.7)	202 (8)^d	210.8	218^e
				215^f
K^+(Phe)	150.5 (5.8)		140.8	145^e
K^+(Tyr)	155.3 (8.7)		142.5	145^e
K^+(Trp)	165.0 (5.8)		153.4	157^e
Na^+(glycine)	164.0 (4.8)^g			
Na^+(benzene)	95.3 (5.7)^h			
Na^+(phenol)	100.4 (4.8)^i			
Na^+(indole)	121.8 (4.8)^j			
K^+(glycine)	121.3 (4.5)^k			
K^+(benzene)	73.3 (3.8)^l			
K^+(phenol)	74.0 (3.4)^m			
K^+(indole)	99.6 (3.9)^j			

^{a} Threshold collision-induced dissociation, present results except as noted. ^{b} B3LYP/6-311++G(3df,3pd)//B3LYP/6-31G* including ZPE and BSSE corrections, present results. ^{c} Equilibrium method, ref 42. ^{d} Equilibrium method, ref 46. ^{e} B3LYP/6-31+G* including ZPE and BSSE corrections, ref 41. ^{f} B3P86/6-31+G* including ZPE and BSSE corrections, ref 42. ^{g} Reference 76. ^{h} Reference 26. ^{i} Average value from refs 20 and 32. ^{j} Reference 35. ^{k} Reference 77. ^{l} Reference 25. ^{m} Reference 32.

ion–molecule complexes.[20,25,28−32,34,36,50,66,74,75] Good reproduction of the data is obtained over energy ranges exceeding 3.5 eV and cross section magnitudes of at least a factor of 100. Table 1 also lists values of E_0 obtained without including the RRKM lifetime analysis. Comparison of these values with the E_0(PSL) values shows that the kinetic shifts for the K^+ systems vary between 0.39 and 0.81. As expected for the more strongly bound Na^+ systems, the kinetic shifts are larger and vary between 0.89 and 1.37. The total number of vibrations changes for these three $M^+(AAA)$ complexes (66 for M^+(Phe), 69 for M^+(Tyr), and 78 for M^+(Trp)), which explains the observed trend in the kinetic shifts: Phe < Tyr < Trp for the complexes to both alkali metal cations.

The entropy of activation, $\Delta S^\ddagger$, is a measure of the looseness of the TS and also a reflection of the complexity of the system. It is calculated using standard formulas and the vibrational frequencies and rotational constants (assuming harmonic oscillator and rigid rotor models) of the energized molecule and the TS for dissociation as listed in Table 1S and 2S. The $\Delta S^\ddagger$ (PSL) values at 1000 K are listed in Table 1 and vary from 48 to 61 J/K mol and are slightly larger for the $Na^+(AAA)$ complexes than the $K^+(AAA)$ complexes. These values are somewhat larger than typical $\Delta S^\ddagger$ values at 1000 K for other noncovalently bound complexes compiled by Lifshitz[73] and previously studied in our laboratory, but are of similar magnitude to those we observed for M^+(adenine) complexes.[74,75] This is easily understood because multidentate binding in the $M^+(AAA)$ and M^+(adenine) complexes should result in larger entropy changes upon dissociation than for complexes that involve monodentate binding.

Theoretical Results. Theoretical structures for Phe, Tyr, and Trp and for the complexes of these AAAs with Na^+ and K^+ were calculated as described above. Table 3 provides key geometrical parameters of the optimized geometries for each

(73) Lifshitz, C. *Adv. Mass Spectrom.* **1989**, *11*, 113.
(74) Rodgers, M. T.; Armentrout, P. B. *J. Am. Chem. Soc.* **2000**, *122*, 8548.
(75) Rodgers, M. T.; Armentrout, P. B. *J. Am. Chem. Soc.* **2002**, *124*, 2678.
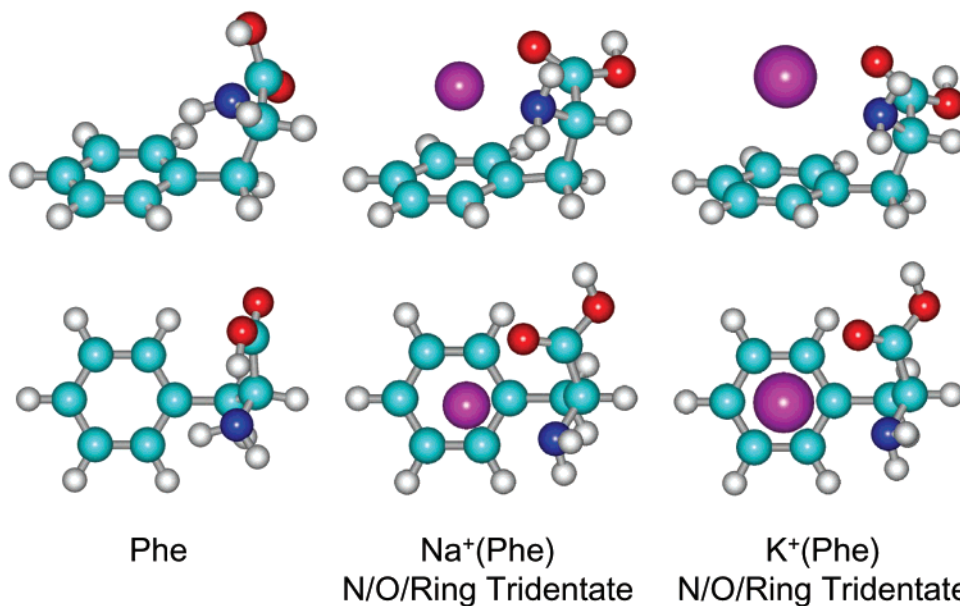
Figure 3. Ground-state B3LYP/6-31G* optimized geometries of Phe, Na+(Phe), and K+(Phe). Two views of each structure are shown.
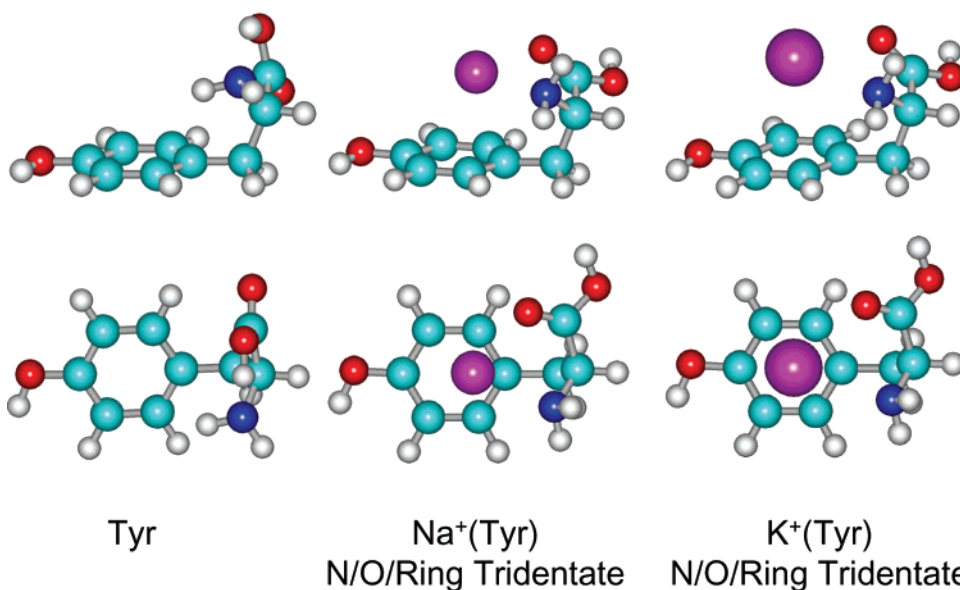

Figure 4. Ground-state B3LYP/6-31G* optimized geometries of Tyr, Na+(Tyr), and K+(Tyr). Two views of each structure are shown.

Table 3. Geometrical Parameters of Ground-State B3LYP/6-31G* Optimized Structures of AAA and M+(AAA) Complexes

species	M+−O (Å)	C=O (Å)	M+−N (Å)	C−N (Å)	M+−R⊥ (Å)	M+−Rc (Å)	offset (Å)	-∠NCC (deg)	-∠OCC (deg)	-∠CCC (deg)	-∠NCCC (deg)
Phe		1.211		1.473				108.7	123.1	113.9	52.3
Na+(Phe)	2.301	1.224	2.447	1.477	2.623	2.684	0.569	107.8	124.3	113.7	53.7
K+(Phe)	2.660	1.220	2.904	1.473	3.018	3.033	0.307	108.7	125.1	114.6	55.8
Tyr		1.211		1.473				108.7	123.1	114.1	52.2
Na+(Tyr)	2.299	1.224	2.443	1.477	2.619	2.693	0.629	107.9	124.3	114.2	52.9
K+(Tyr)	2.655	1.220	2.897	1.474	3.022	3.042	0.350	108.7	125.2	114.9	55.5
Trp		1.212		1.474				108.5	123.2	113.5	55.6
Na+(Trp)	2.294	1.223	2.429	1.477	2.558	3.064	1.687	108.1	124.5	115.9	72.7
K+(Trp)	2.532	1.223	5.957	1.471	2.949	2.965	0.309	107.2	123.4	115.9	175.2

of these systems. Detailed geometries are also provided in the Supporting Information in Table 3S. Structures of the most stable conformations of the neutral AAAs and their complexes to Na+ and K+ are shown in Figures 3−5 for the Phe, Tyr, and Trp systems, respectively. The 0 K calculated alkali metal cation binding energies, performed at the B3LYP/6-311++G(3df,-

3pd)//B3LYP/6-31G* level of theory including ZPE and BSSE corrections, are listed in Table 2.

In earlier work, Dunbar explored the complexation of Na+ and K+ to Phe, Tyr, and Trp.[41] Various low-energy conformations of the neutral AAAs and the M+(AAA) complexes were explored and characterized energetically. Theoretical estimates
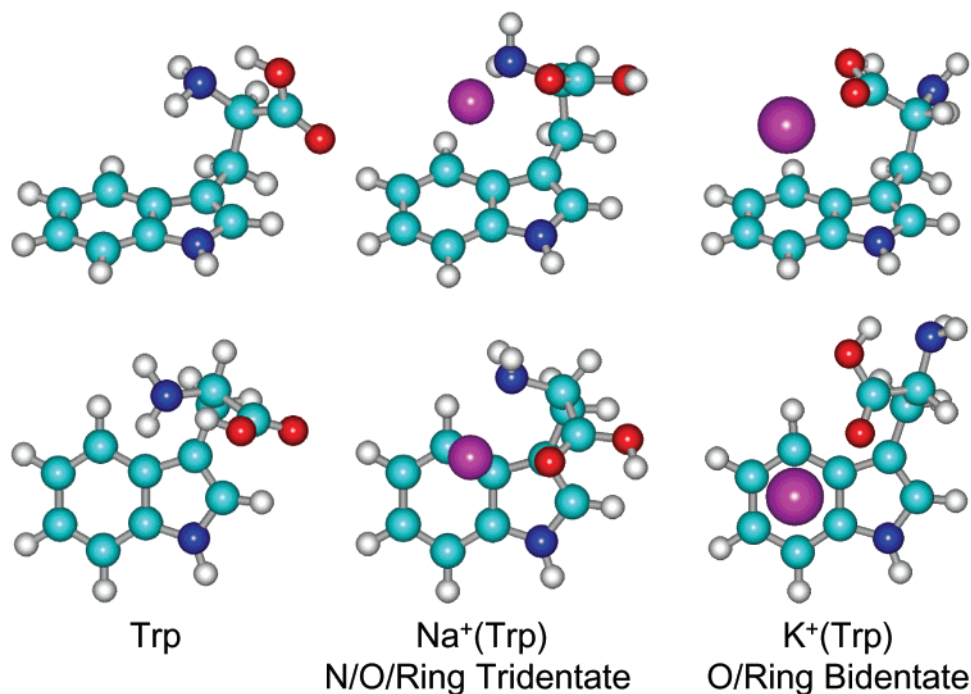
Figure 5. Ground-state B3LYP/6-31G* optimized geometries of Trp, Na$^+$(Trp), and K$^+$(Trp). Two views of each structure are shown.

for the strength of binding in the M$^+$(AAA) complexes were then calculated on the basis of the most stable structures found. In a later study, Gapeev and Dunbar[42] re-examined the conformational space of neutral Phe and identified a conformation that was calculated to be ~8.4 kJ/mol more stable than the lowest-energy structure previously reported. This latter work dealt only with the complexation of Na$^+$ to Phe, and therefore a revised value for the Na$^+$(Phe) BDE was reported. Revised values for the other M$^+$(AAA) BDEs were not reported. The theoretical M$^+$(AAA) BDEs determined by Dunbar and co-workers are also listed in Table 2.[41,42] The optimized structures reported in both of these studies were shown pictorially with key geometrical parameters provided. However, full details of the optimized geometries were not provided. Thus, the discussion below is somewhat qualitative and based upon the limited information provided in those studies.

Neutral AAAs. The lowest-energy conformations of Phe, Tyr, and Trp identified in the present work all have similar backbone conformations, Figures 3–5, in which additional stabilization is gained through a hydrogen bond between the hydroxyl H atom and the amino N atom as well as through interaction of one of the amino H atoms with the aromatic ring. These structures are analogous to the lowest-energy conformer of Phe identified by Gapeev and Dunbar,[42] but represent new lower-energy conformations of Tyr and Trp than previously reported. The difference in the stability of the lowest-energy conformers determined here and those analogous to the structures originally reported by Dunbar are 4.8, 4.6, and 7.0 kJ/mol (2.9, 2.6, and 5.1 kJ/mol including ZPE corrections). These results suggest that the theoretical BDEs derived by Dunbar in his original work for all of the M$^+$(AAA) complexes should be lowered appropriately. Because a slightly different level of theory has been employed in the present work, Dunbar's values reported in Table 2 have not been adjusted.

M$^+$(AAA) Complexes. The calculations find that the preferred binding geometry of all of the M$^+$(AAA) complexes

except K$^+$(Trp) involve tridentate binding to the carbonyl O atom, the amino N atom, and to the π cloud of the aromatic ring, Figures 3–5. The optimized geometries of the M$^+$(Tyr) complexes are very similar to Phe and the M$^+$(Phe) complexes, suggesting that the hydroxyl substituent does not significantly influence the binding. In contrast to that found for all of the other M$^+$(AAA) complexes, the K$^+$(Trp) complex prefers bidentate binding to the carbonyl O atom and the aromatic ring. The structures of all of these complexes are similar to the lowest-energy conformations previously reported by Dunbar.[41] However, the alkali metal cation–ligand bond distances are slightly shorter than previously found. These binding geometries comprise the combination of binding modes found for Glycine (Gly), the simplest amino acid having no side chain, and that observed for the side chain aromatic ligands, benzene, phenol, and indole.[25,32,35,76,77] However, geometric constraints within the AAA ligand do not allow the alkali metal cation to optimally interact with each of these functional groups as seen by comparing the binding geometry of the M$^+$(AAA) complexes to those found for the M$^+$(Gly), M$^+$(benzene), M$^+$(phenol), and M$^+$(indole) complexes.

The ground-state conformation of Na$^+$(Gly) involves bidentate binding to the carbonyl O atom and the amino N atom.[76] In the Na$^+$(AAA) complexes, these interactions are maintained but influenced by the additional chelation interaction with the aromatic side chain. In the Na$^+$(AAA) complexes, the Na$^+$–O bond distance increases by 0.033 to 0.040 Å as compared to Na$^+$(Gly). In contrast, the Na$^+$–N bond distance is altered to a much lesser extent, increasing by 0.002 Å in Na$^+$(Phe) and decreasing by 0.002 and 0.016 Å in the Na$^+$(Tyr) and Na$^+$-(Trp) complexes, respectively. In their dissection of the Na$^+$-(Gly) interactions, Moision and Armentrout[76] determined that the interaction of the alkali metal cation with the carbonyl O atom contributes more to the binding than the interaction with

(76) Moision, R. M.; Armentrout, P. B. *J. Phys. Chem. A* **2002**, *106*, 10350.
(77) Moision, R. M.; Armentrout, P. B. *Phys. Chem. Chem. Phys.* **2004**, *6*, 2588.

the amino N atom. This conclusion is also supported by the relative Na⁺−O and Na⁺−N bond distances. Thus, it is not surprising that the Na⁺−O bond distance is more profoundly influenced by interaction of Na⁺ with the aromatic side chain in the Na⁺(AAA) complexes.

The interaction of the alkali metal cation with the aromatic side chain in the Na⁺(AAA) complexes is much less ideal than in the isolated Na⁺(benzene), Na⁺(phenol), and Na⁺(indole) complexes. In the Na⁺(benzene) complex, Na⁺ sits directly above the center of the aromatic ring. In the Na⁺(Phe) complex, the perpendicular distance between Na⁺ and the aromatic ring, Na⁺−R⊥ increases by 0.250 Å and is offset from the center of the ring by 0.569 Å as compared to Na⁺(benzene). Two nearly isoenergetic stable conformations are observed for the Na⁺-(phenol) complex. The first of these conformations is analogous to that found for Na⁺(benzene) in that Na⁺ sits directly above the center of the aromatic ring and the hydroxyl substituent lies in the plane of the aromatic ring. In the second conformation, Na⁺ lies above the plane of the aromatic ring and is located between the two lone pairs of electrons on the O atom of the hydroxyl substituent. This latter binding conformation is not favorable for the Na⁺(Tyr) complex because steric constraints would not allow additional stabilization via interaction with the amino acid backbone. In the Na⁺(Tyr) complex, Na⁺−R⊥ increases by 0.246 Å and is offset from the center of the ring by 0.629 Å as compared to the Na⁺(phenol) cation−π complex. Two stable conformations are also found for the Na⁺(indole) complex.[35] In the ground-state conformation, Na⁺ sits above the six-membered ring, but is offset from the ring centroid by 0.179 Å. In the excited conformation, Na⁺ sits above the five-membered ring but is skewed toward C8. In the Na⁺(Trp) complex, Na⁺ sits above the six-membered ring, but Na⁺−R⊥ increases by 0.219 Å and is further offset from the center of the ring by 1.508 Å as compared to Na⁺(indole). Thus, in the Na⁺(AAA) complexes, it is clear that the binding is dominated by the amino acid backbone and enhanced by additional interaction with aromatic side chain.

The ground-state conformation of the K⁺(Gly) complex differs from that observed for Na⁺(Gly) and is found to be model dependent.[77] DFT optimization of the K⁺(Gly) complex finds that the ground-state conformation involves monodentate binding to the carbonyl O atom, whereas MP2 optimization suggests that the ground state involves bidentate binding to both O atoms of the carboxyl group. These conformations differ by 0−3 kJ/mol depending upon the level of theory employed. In contrast, the conformation of K⁺(Gly) analogous to that found for the ground state of Na⁺(Gly) (i.e., bidentate binding to the carbonyl O atom and the amino N atom) lies 1−7 kJ/mol above the ground-state conformation. In the K⁺(Phe) and K⁺(Tyr) complexes, this latter mode of binding is most favorable. As found in the Na⁺(AAA) complexes, the alkali metal cation−carbonyl O interaction is influenced more significantly than the interaction with the amino N atom. The K⁺−N and K⁺−O bond distances increase as compared to the analogous low-lying excited conformer of K⁺(Gly), by 0.024 and 0.046 Å for K⁺(Phe) and by 0.017 and 0.041 Å, respectively. Again, the interaction with the aromatic side chain is not ideal. The K⁺−R⊥ distance in the K⁺(Phe) and K⁺(Tyr) complexes increases by 0.177 and 0.175 Å and is offset from the center of the ring by 0.307 and 0.350 Å as compared to K⁺(benzene) and K⁺(phenol).[25,32] The

change in preferred binding mode to the backbone, the larger differences in the M⁺−N and M⁺−O distances, the smaller difference in the M⁺−R⊥ distance, and the smaller offset all suggest that the interaction with the aromatic side chain contributes more to the binding in these K⁺(AAA) complexes than in the analogous Na⁺(AAA) complexes.

In the K⁺(Trp) complex, the interaction of K⁺ with the amino acid backbone is analogous to that found for the DFT ground-state conformation (i.e., mondentate binding to the carbonyl O atom). In the K⁺(Trp) complex, the K⁺−O bond distance decreases as compared to K⁺(Gly) by 0.022 Å. The interaction of the alkali metal cation with the aromatic side chain in K⁺-(Trp) is much more favorable than found for Na⁺(Trp). Two stable conformations are also found for the K⁺(indole) complex.[35] In the ground-state conformation, K⁺ sits above the six-membered ring, but is offset from the ring centroid by 0.161 Å. In the K⁺(Trp) complex, K⁺ also sits above the six-membered ring, but the K⁺−R⊥ increases by 0.127 Å and the offset from the center of the ring increases by 0.148 Å as compared to the K⁺(indole) complex.[35] Thus, it is again clear that the interaction with the aromatic side chain contributes more to the binding in the K⁺(Trp) complex than in the Na⁺(Trp) complex. The more favorable K⁺−aromatic interactions likely arise as a result of its larger size leading to less steric problems and more effective acceptance of the diffuse π electron density of the aromatic ring.

Analysis of the structures of the Na⁺(Phe) complex obtained when geometry optimizations are performed using different basis sets indicated that the optimal mode of binding is slightly influenced by the basis set chosen. The M⁺−O and M⁺−N bond distances increase from 2.278 to 2.306 Å and 2.419 to 2.457 Å, respectively, as the basis set is varied from 6-31G to 6-31+G to 6-31G* to 6-31+G*. In contrast, the M⁺−R⊥, M⁺−R_C, and the offset of the metal ion from the center of the aromatic ring increase from 2.623 to 2.769 Å, 2.684 to 2.897 Å, and 0.569 to 0.853 Å, respectively, as the basis set is varied from 6-31G* to 6-31G to 6-31+G* to 6-31+G. The relative stabilities of the Na⁺(Phe) complexes determined from single-point energy calculations at the B3LYP/6-311++G(3df,3pd) level of theory using the 6-31G*, 6-31+G*, 6-31G, and 6-31+G optimized geometries are 0.0, 0.1, 9.5, and 10.5 kJ/mol. Thus, geometry optimization using the 6-31G* basis set, as was used for all of the neutral AAAs and the M⁺(AAA) complexes in this work, provides the most favorable description of the alkali metal cation−AAA interaction.

Discussion

Comparison of Theory and Experiment. The Na⁺ and K⁺ cation affinities of Phe, Tyr, and Trp at 0 K measured by TCID in a guided ion beam mass spectrometer and calculated here are summarized in Table 2. The agreement between theory and experiment is illustrated in Figure 6. Measured values obtained using the equilibrium method and theoretical values from the literature are also included in Table 2 and Figure 6 for comparison.[41,42,44,46] It can be seen that the agreement between theory and the TCID experimental results is very reasonable over the nearly 70 kJ/mol variation in the alkali metal cation binding affinities measured here. In all cases, the measured BDEs are greater than the calculated values. For the six M⁺-(AAA) systems, the mean absolute deviation (MAD) between theory and experiment is 10.2 ± 2.3 kJ/mol, somewhat larger
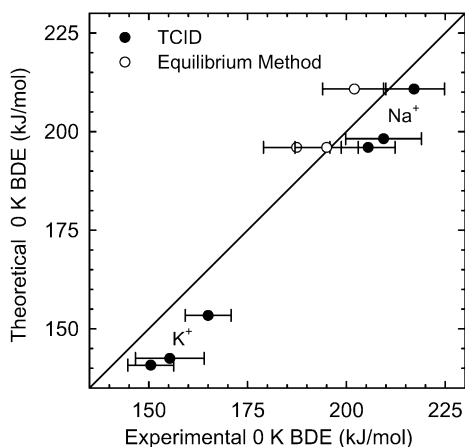
Figure 6. Theoretical versus experimental 0 K bond dissociation energies of M^+−AAA (in kJ/mol), where M^+ = Na^+ and K^+ and AAA = Phe, Tyr, Trp. Experimental results include values measured here, TCID (●), as well as values from equilibrium measurements (○, refs 42 and 46).

than the average experimental error in these values, 7.4 ± 1.6 kJ/mol. However, the MAD is within the expected computational accuracy for this level of theory.[20] It can therefore be concluded that the BDEs measured here for the aromatic amino acids can act as reliable anchors for the alkali metal cation affinity scales.

Comparison of TCID and Ligand Exchange Equilibrium Results. Ligand exchange equilibrium measurements have only been made for the Na^+(Phe) and Na^+(Trp) complexes. The Na^+-(Phe) BDE determined in the initial study by Gapeev and Dunbar is 18.1 kJ/mol lower than the value measured here, but only 8.6 kJ/mol lower than the calculated value.[42] In their more recent study, Gapeev and Dunbar measured the Na^+(Trp) binding affinity and remeasured the Na^+(Phe) binding affinity.[46] The remeasured value for Na^+(Phe) was 8 kJ/mol larger than that found in their previous study and therefore 10.1 kJ/mol lower than the value measured here and only 0.6 kJ/mol lower than the calculated value, suggesting that this latter determination is more accurate. The value determined for Na^+(Trp) is 15.1 kJ/mol lower than the value measured here, but only 8.8 kJ/mol lower than the calculated value.[46] Equilibrium methods are a very well-established part of thermodynamics. However, to extract the BDE, entropy corrections must be made. The entropy corrections rely on molecular parameters determined from theoretical calculations and are found to be quite substantial for these systems, ∼16 kJ/mol. Although Gapeev and Dunbar include assessments of uncertainties in the entropy corrections in the uncertainties reported for the absolute sodium ion affinities, details of the magnitudes of these corrections were not discussed. Furthermore, equilibrium can be difficult to achieve when working with such nonvolatile species, and the accurate measurement of vapor pressures of the species involved is difficult. This may explain why the measured BDE for Na^+-(Phe) differed in these two studies.

Comparison of TCID and Kinetic Method Results. Although kinetic method measurements have been made for all of the systems examined here,[44,45] comparison with those results is complex and hence has been moved to the Supporting Information to avoid distractions from the main issues being addressed in the current manuscript.

Trends in the Binding of Na^+ and K^+ to the Aromatic Amino Acids. In the M^+(AAA) systems examined here, the measured binding strength varies with the alkali metal cation such that Na^+ binds 36.5%, 34.8%, and 31.5% more strongly than K^+ in the Phe, Tyr, and Trp complexes, respectively. This can be explained on the basis of electrostatic ideas. The alkali metal cations have s^0 electron configurations and thus spherically symmetric electron densities. The alkali metal cation−ligand bond lengths are mainly determined by the size of cation such that the larger the radius, the longer the bond distances and the weaker the interactions. The ion−dipole, ion−quadrupole, and ion−induced dipole interactions of K^+ with the aromatic amino acids are therefore weaker than for Na^+, resulting in lower binding energies.

It is interesting to note that all of the M^+(AAA) complexes involve tridentate binding except the K^+(Trp) complex, which is bidentate, yet the Trp complexes exhibit the smallest percent increase in the binding affinity of Na^+ versus K^+. At first glance, it might be expected that the reverse trend would be observed, that is, that a greater enhancement in the binding energy would be seen for Na^+(Trp) as compared to K^+(Trp) than for Phe and Tyr because less interactions occur for the K^+(Trp) complex. However, in all cases except the K^+(Trp) complex, the cation−π interaction is less than ideal and the alkali metal cation is further from the aromatic ring and offset from the center of the ring as compared to benzene, phenol, and indole. Thus, it appears that the more ideal cation−π interaction in the K^+(Trp) complex just slightly more than compensates for the decrease in the number of alkali metal cation−chelation interactions.

The Mulliken charge retained by the metal cations in the M^+-(AAA) complexes is lower for the Na^+ complexes, ∼0.59e, than for the K^+ complexes, ∼0.77e. This confirms the electrostatic nature of the M^+−AAA binding, but also suggests that there is significant covalency in the binding as a result of charge transfer, especially for the Na^+ complexes. The shorter metal−ligand bond lengths and greater charge density on Na^+ allow it to more effectively withdraw electron density from the aromatic amino acid. The multidentate binding leads to a much greater level of charge transfer than is typically found for monodentate binding to these alkali metal cations, and more akin to that observed in multiply ligated complexes, M^+L_x.[78]

Influence of the Side-Chain Substituent. The effect that the side chain has upon the binding can be examined by comparing these systems to the simplest amino acid, Gly. In all cases, the BDEs of the six M^+(AAA) complexes are larger than those for the corresponding M^+(Gly) complexes, Table 2. This is the expected trend based upon the structures determined for these M^+(AAA) complexes, where the alkali metal cation binds to the amino acid backbone and gains additional stabilization through interaction with the side-chain substituent. The enhancement in the binding is found to depend both on the alkali metal cation and on the side chain of the AAA. The enhancements in the binding for the Na^+ complexes (41.5, 45.4, and 53.1 kJ/mol) are greater than those for the corresponding K^+ complexes (29.2, 34.0, and 43.7 kJ/mol) to Phe, Tyr, and Trp, respectively. As can be seen above, the enhancement in the binding increases from Phe to Tyr to Trp for both alkali metal cations. The former arises because these are electrostatically

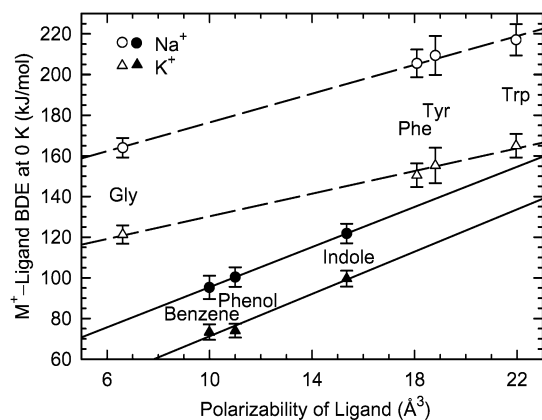(78) Valina, A. B.; Amunugama, R.; Huang, H.; Rodgers, M. T. *J. Phys. Chem. A* **2001**, *105*, 11057.

Figure 7. Measured M$^+$−ligand BDEs at 0 K (in kJ/mol) versus estimated polarizability[75] of the ligand. Values are shown for M$^+$ = Na$^+$ and K$^+$, and ligand = Phe, Tyr, Trp, benzene phenol, and indole. Lines are linear regression fits to the data for each alkali metal carbon and series of ligands.

bound complexes whose binding energies are strongly dependent upon the alkali metal cation−ligand bond distances as discussed above. The trends among the three AAAs arise as a result of the influence of the side-chain substituent. The polarizability of Gly is estimated to be 6.61 Å^3 and increases to 18.09 Å^3 for Phe, 18.81 Å^3 for Tyr, and 21.96 Å^3 for Trp.[79] As can be seen in Figure 7, a very good linear correlation between the measured BDEs for M$^+$(Gly) and the M$^+$(AAA) complexes and the polarizabilities of the neutral amino acids is found for each alkali metal cation. This suggests that the polarizability of the amino acid is a key factor in determining the strength of the binding in these systems.

Based upon the optimized structures of the M$^+$(AAA) complexes, as well as the increase in the measured BDES of these complexes as compared to the corresponding M$^+$(Gly) complexes, it is clear that the alkali metal cation is unable to achieve optimal binding to both the amino acid backbone and the aromatic side-chain substituent. Comparison of the M$^+$-(AAA) BDEs to the sum of the corresponding M$^+$(Gly) and M$^+$(arene) complexes, where arene = benzene, phenol, and indole, shows that the M$^+$(AAA) complexes recover 75−80% of the binding. As has been found in numerous previous studies, a monotonic decrease in the binding energies is observed upon sequential ligation of alkali metal cations.[21,25,29−34,36,37,52,56,78] The observed decrease in the binding energies arises as a result of repulsive ligand−ligand interactions. The magnitude of the decrease in the binding strength therefore depends on both the size and the binding geometry of the ligands, but typically results in weaker binding of the second ligand by approximately 5−20% as compared to the first ligand. Therefore, the steric limitations associated with the covalent binding between the amino acid backbone and the aromatic side-chain substituent probably only cost about 20−40 kJ/mol. The energetic costs are larger for Na$^+$ than K$^+$ as a result of the strong binding and smaller size of the cation as seen by the larger deviations from the ideal cation−π interaction between the alkali metal cation and the aromatic side-chain substituent as discussed above and summarized in Table 3.

Trends in the Binding of Alkali Metal Cations to the Aromatic Amino Acids. The measured and calculated M$^+$−AAA BDEs follow the order Phe < Tyr < Trp for the

complexes to both Na$^+$ and K$^+$. As discussed above, the binding in these complexes is dominated by the interaction with the amino acid backbone and enhanced by interaction with the side-chain substituent. Therefore, in examining the trends among the AAAs, it is appropriate to examine the trends in the binding of the isolated aromatic ligands: benzene, phenol, and indole. The variation in BDEs for these ligands can again be understood on the basis of electrostatic ideas. In a study of Na$^+$ binding to 11 aromatic systems, Mecozzi and Dougherty[80] found good correlation between the strength of the cation−π interaction and the charge-permanent quadrupole term of the electrostatic potential. Therefore, they concluded that the variation in cation−π binding energies are faithfully mirrored by the charge-permanent quadrupole term of the molecular electrostatic potential (MEP), and this has been quantitatively supported.[4] However, Cubero and Orozco pointed out that polarization is also important in cation−π interactions. They developed a generalized molecular interaction potential with polarization (GMIPp), including MEP, classical dispersion−repulsion, and a polarization term derived from perturbation theory.[24] The GMIPp model is able to better explain the difference in binding energy of Na$^+$ to benzene and naphthalene than Dougherty's MEP model. In previous work from our group, we have also found that both the ion−quadrupole and the ion−induced dipole interactions needed to be considered to explain the trends in the BDEs of M$^+$(arene) complexes, where arene = benzene, pyrrole, toluene, fluorobenzene, aniline, phenol, anisole, and naphthalene.[25,28−32,34,36]

Trends in the Binding of Alkali Metal Cations to Benzene, Phenol, and Indole. The BDEs of M$^+$(arene), where M$^+$ = Na$^+$ and K$^+$ and arene = benzene, phenol, and indole, are also given in Table 2. Although more than one literature value is available for several of these systems, for consistency with the present results, we will only compare to other TCID values. As can be seen from Table 2, the BDEs of these complexes follow the order M$^+$(benzene) < M$^+$(phenol) < M$^+$(indole) for both Na$^+$ and K$^+$. This parallels the measured BDEs for the corresponding M$^+$(AAA) complexes, M$^+$(Phe) < M$^+$(Tyr)) < M$^+$(Trp). The differences in the measured BDEs to benzene and phenol are small and generally smaller than the experimental error in these measurements, suggesting that the relative binding affinities of benzene and phenol may not be accurately known. However, competitive dissociation of M$^+$(benzene)(phenol) complexes clearly indicates that the binding to phenol is stronger than that to benzene.[81] The trends among these three aromatic ligands can therefore be understood on the basis of the quadrupole moments and polarizabilities of these ligands. The polarizability of benzene is estimated to be 9.99 Å^3 and increases to 11.00 Å^3 for phenol and to 15.35 Å^3 for indole. As can be seen in Figure 7, a very good linear correlation between the measured M$^+$(arene) BDEs and the polarizabilities of the neutral ligands is found for each alkali metal cation. This again suggests that the polarizability of the ligand is a key factor in determining the strength of the binding in these systems. As can also be seen in Figure 7, the correlation between the binding energies and the polarizabilities is very different for the amino acids than for the aromatic ligands. Thus, the binding in the M$^+$(AAA) complexes is dominated by interaction with the amino acid

(79) Miller, K. J. *J. Am. Chem. Soc.* **1990**, *112*, 8533.

(80) Mecozzi, S.; West, A. P.; Dougherty, D. A. *J. Am. Chem. Soc.* **1996**, *118*, 2307.

(81) Ditri, T. B.; Rodgers, M. T., unpublished results.

backbone as suggested above. The fact that the M⁺(arene) BDEs increase more rapidly with polarizability than for the M⁺(AAA) complexes suggests that the ion−quadrupole interaction plays a larger role in the former complexes. The quadrupole moment of benzene has been measured, −8.69 DÅ.[82] Unfortunately, the quadrupole moment can only be measured for compounds that have no dipole moment. However, it has been estimated that the hydroxyl substituent leads to a small increase, ∼0.1 DÅ, in the quadrupole moment as compared to benzene.[36] Although indole was not included in the previous analysis,[36] the larger size of the aromatic ring system as well as the presence of electron-rich nitrogen atom should both contribute to an enhancement in the quadrupole moment of indole as compared to benzene. Thus, both the ion−quadrupole and the ion−induced dipole interactions should lead to the strongest cation−π interactions for indole followed by phenol and then benzene. Thus, for a given alkali metal cation, both the ion−quadrupole and the ion−induced dipole interactions with the side chain should follow the order Phe < Tyr < Trp as observed.

Conclusions

The kinetic energy dependence of the CID of M⁺(AAA), where M⁺ = Na⁺ and K⁺ and AAA = Phe, Tyr, and Trp, with Xe is examined in a guided ion beam tandem mass spectrometer. The only dissociation pathway observed in these noncovalently bound complexes is loss of the intact aromatic amino acid. Thresholds for these CID processes are determined after consideration of the effects of the kinetic energy distributions of the reactants, the internal energy distribution of the reactant ion, multiple collisions with Xe, and the lifetime for dissociation. Insight into the structures and binding of the alkali metal ion to the aromatic amino acids is provided by density functional theory calculations of these complexes performed at the B3LYP/6-311++G(3df,3pd)//B3LYP/6-31G* level of theory. New lower-energy conformers of Tyr and Trp were found, suggesting that the previously reported theoretical BDEs should be lowered. The calculated BDEs are systematically lower than the measured values by 10.2 ± 2.3 kJ/mol. This is within the expected

accuracy of this level of theory and therefore represents reasonable agreement. Thus, it can be concluded that the BDEs measured here for the aromatic amino acids can act as reliable anchors for the alkali metal cation affinity scales and can broaden the range of ligands available as absolute thermochemical anchors. The BDEs determined in the ligand exchange equilibrium studies for Na⁺(Phe) and Na⁺(Trp) are also lower than the values measured here, by 10.1 and 15.1 kJ/mol, respectively.

Although the aromatic side chain is found to enhance the BDEs of the M⁺(AAA) complexes, the binding in these complexes is clearly dominated by interactions with the amino acid backbone. Therefore, it is inappropriate to think of these M⁺(AAA) complexes merely in terms of cation−π complexes. This may differ from the behavior of such interactions in large peptides and proteins where the amino acid backbone may be less accessible to the cation as a result of folding of the peptide or protein. In this sense, the model studies performed may provide more detailed and fundamental insight into the nature of cation−π interactions in real biological systems. However, the preferential cleavage of alkaline earth metal cation bound peptides adjacent to aromatic amino acid residues suggests that the amino acid backbone of these particular peptides is accessible to the metal cations. Therefore, data obtained from model systems and the aromatic amino acids complement each other and provide a more detailed understanding of the interaction between alkali metal cations and peptides or proteins.

Supporting Information Available: Tables of vibrational frequencies and average vibrational energies at 298 K, rotational constants, B3LYP/6-31G* optimized geometries, and enthalpies and free energies at 298 K; figures giving cross sections for collision-induced dissociation and thermochemical analyses of collision-induced dissociation cross sections, and a comparison of TCID and kinetic method results. This material is available free of charge via the Internet at http://pubs.acs.org.

(82) Williams, J. H. *Acc. Chem. Res.* **1993**, *26*, 593.

JA048297E